Robust and time-resolved estimation of cardiac sympathetic and parasympathetic indices

Diego Candia-Rivera*, Fabrizio de Vico Fallani, and Mario Chavez

Abstract— **The time-resolved analysis of heart rate (HR) and heart rate variability (HRV) is crucial for the evaluation of the dynamic changes of autonomic activity under different clinical and behavioral conditions. Standard HRV analysis is performed in the frequency domain because the sympathetic activations tend to increase low-frequency HRV oscillations, while the parasympathetic ones increase high-frequency HRV oscillations. However, a strict separation of HRV in frequency bands may cause biased estimations, especially in the low frequency range. To overcome this limitation, we propose a robust estimator that combines HR and HRV dynamics, based on the correlation of the Poincaré plot descriptors of interbeat intervals from the electrocardiogram. To validate our method, we used electrocardiograms gathered from different open databases where standardized paradigms were applied to elicit changes in autonomic activity. Our proposal outperforms the standard spectral approach for the estimation of low- and high-frequency fluctuations in HRV, which are mostly triggered by sympathetic and parasympathetic activity, respectively. Our method constitutes a valuable, robust, time-resolved, and cost-effective tool for a better understanding of autonomic activity through HR and HRV in healthy state and potentially for pathological conditions.**

I. Introduction

THE analysis of autonomic dynamics through heart rate variability (HRV) is a standard approach for clinical and fundamental research [1]–[3]. Biomarkers based on HRV serve for the non-invasive analysis of physiological responses to different stimuli, which allows the assessment of several pathological conditions [4]–[6]. Additionally, HRV analysis can enable the characterization of neural processes, which can help to enlighten the physiological underpinnings behind homeostatic regulations, sensorimotor function, and cognition [7].

Heartbeats are generated from the continuous interactions within the autonomic nervous system, between sympathetic and parasympathetic outflows [8]. These interactions occur specifically on the sinoatrial node, which contains the pacemaker cells that contract to produce the heartbeats [9]. The fluctuations in the autonomic modulations to the sinoatrial node cause the heartbeat generation at different rhythms [10], as a function of the sympathetic and parasympathetic activations that cause changes in the release rate of noradrenaline and acetylcholine [11]. The estimation of the sympathetic and parasympathetic activities is usually performed through HRV spectral integration at the low- (LF: 0.04–0.15 Hz) and high-frequency (HF: 0.15–0.4 Hz), respectively [12], [13]. However, the spectral components of HRV series can be biased in certain conditions [14]. Specifically, the fixed subdivisions for the frequency ranges (LF and HF) cannot successfully separate the influences of the ongoing sympathetic and parasympathetic activities, which are potentially overlapped in the LF range [1]. To overcome this issue, alternative strategies have been proposed to estimate autonomic dynamics and to disentangle the low and high-frequency HRV oscillations [15]–[18].

We propose a method for a robust estimation of sympathetic and parasympathetic activities. The method is grounded on the measurement of the successive changes in interbeat intervals, by analyzing the changes of the Poincaré plot geometry over time. Our approach demonstrates its ability to precisely estimate cardiac sympathetic and parasympathetic responses in healthy subjects during postural changes and a cold-pressor test, standard autonomic stimulation protocols. Our method holds potential for the future development of biomarkers for clinical conditions related to dysautonomia.

II. Materials and Methods

A. Datasets description

Twenty-four adults were recruited for the cold-pressor test. A total of 18 subjects were included in this study (six of them were discarded because of missing data in their ECG). Three trials of the cold pressor test were performed. Each trial consisted in a 5-minute resting period, followed by a 3-minute immersion of the hand in ice water (0°C) and a 2-minute recovery through immersion of the same hand in warmer water (32°C). In this study, the first trial was considered. Trials were considered in the -120 to 120 s with respect the onset of the cold-pressor test. ECG was measured using Finapres NOVA system (Finapres Medical Systems, Amsterdam, The Netherlands) with a sampling frequency of 200 Hz. The study was approved by the local ethical committee (Radboud University, ECS17022 and REC18021). All participants signed informed consent to participate in the study as required by the Declaration of Helsinki. For further detail on the experimental procedures, please refer to the original study [18].

This research was supported by the French Agence Nationale de la Recherche (ANR-20-CE37-0012-03).

D. C. R., F. D. V. F., and M. C. are with Sorbonne Université, Paris Brain Institute (ICM), CNRS-UMR722, INRIA-Paris (Nerv-Team), INSERM-U1127, AP-HP Hôpital Pitié Salpêtrière, F75013, Paris, France. *Correspondence e-mail: diego.candia.r@ug.uchile.cl.

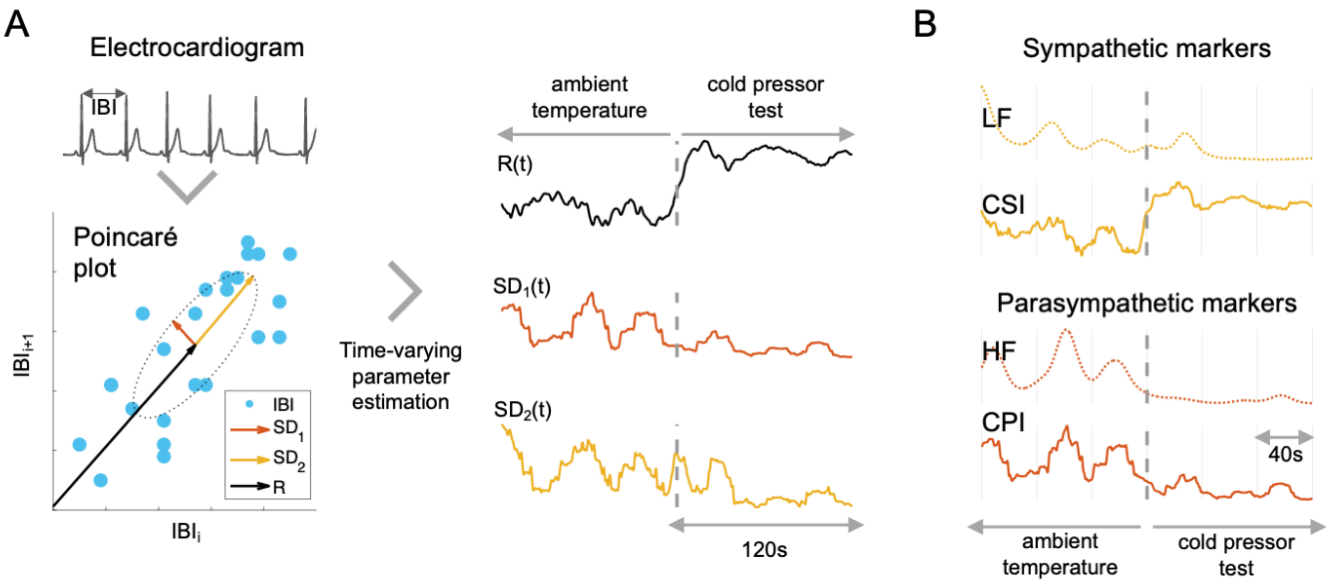

Fig. 1. Estimation of the fluctuating parameters of the Poincaré plot. (A) The Poincaré plot illustrates the sequential changes in interbeat intervals (IBI). It allows us to estimate the Cardiac sympathetic (CSI) and parasympathetic indices (CPI) by calculating the minor (SD1) and major ratios (SD2) of the formed ellipse and the distance (R) from its center to the origin. (B) The estimated CSI and CPI are presented alongside their corresponding spectral counterparts: the low-frequency (LF) and high-frequency (HF) components of heart rate variability, which are aimed to index sympathetic and parasympathetic activity, respectively.

Ten adults were recruited for the tilt-table test. The subjects were initially asked to remain in a horizontal supine position and to move to a vertical position with the help of either the tilt-table or by self-stand up. The subjects were part of six sessions that were sorted randomly between resting periods: two stand up, two slow tilts (50 s from 0 to 70°), and two fast tilts (2 s from 0 to 70°), while remaining in each condition for approximately 3 min. The entire protocol lasted between 55 and 75 minutes for each participant. ECG was measured using Hewlett-Packard 1500A system (Hewlett-Packard, Palo Alto, California, United States of America) with a sampling frequency of 250 Hz. In this study, the trials performed by each participant were considered as individual measurements and independently of the vertical positioning procedure (tilt table or self-stand up). Trials were considered in the -120 to 120 s with respect the onset of the postural change. The study was approved by the local ethical committee (Massachusetts Institute of Technology, COUHES 2895 and MIT CRC 512). All participants signed informed consent to participate in the study as required by the Declaration of Helsinki. For further detail on the experimental procedures, please refer to the original study [19], [20].

B. Estimation of cardiac sympathetic and parasympathetic indices

The R-peaks from the subject ECGs were detected automatically using a method inspired in the Pan–Tompkins algorithm [21]. Consecutively, the detected R-peaks were manually corrected for misdetections or ectopic beats. Interbeat interval series (IBI) were constructed, based on the R-to-R-peak durations. Poincaré plot was used to depict the fluctuations on the duration of consecutive IBI [22], as shown in Figure 1A. We quantified three features from Poincaré plot: R, SD1 and SD2, which correspond to the distance to the origin, and the ratios of the ellipse representing the short- and long-term fluctuations of HRV, respectively [23]. Figure 1B displays the calculations of the Cardiac Sympathetic Index (CSI) and Cardiac Parasympathetic Index (CPI) for a single subject undergoing a cold-pressor test. These indices are derived by integrating the time-resolved estimates of R, SD1, and SD2. Additionally, these estimates are displayed alongside their spectral counterparts, LF and HF.

The time-varying fluctuations of the distance to the origin and the ellipse ratios were computed with a sliding-time window, as shown in Eq. 1, 2 and 3:

$$R(t) = \sqrt{mean(IBI_{i,\dots,n-1})^2 + mean(IBI_{i+1,\dots,n})^2} \quad (1)$$

$$SD_1(t) = \sqrt{\lambda_{\Omega_t}(1,1)} \quad (2)$$

$$SD_2(t) = \sqrt{\lambda_{\Omega_t}(2,2)} \quad (3)$$

where λ_{Ω_t} is the matrix with the eigenvalues of the covariance matrix of $IBI_{i,\dots,n-1}$ and $IBI_{i+1,\dots,n}$, with $\Omega_t: t - T \leq t_i \leq t$, and n is the length of IBI in the time window Ω_t. The method implementation includes four approaches to compute SD1 and SD2: “exact”, “robust”, “95%” and “approximate”. The exact approach computes the standard covariance matrix giving the covariance between each pair of elements. The robust approach computes the covariance matrix using a shrinkage covariance estimator based on the Ledoit-Wolf lemma for analytic calculation of the optimal shrinkage intensity [24]. The 95% approach computes the covariance matrix using the Fast Minimum Covariance Determinant Estimate [25]. This covariance estimation method selects h observations out of total n. The selection of h fulfills the relationship $h \approx (1 - Outlier) \cdot n$,

with $Outlier = 0.05$. Then the selected points fulfill a standard covariance matrix with the lowest determinant. Finally, the approximate approach computes SD1 and SD2 as follows [16]:

$$SD_1(t) = \sqrt{\frac{1}{2}\, std(IBI'_{\Omega_t})^2} \tag{4}$$

$$SD_2(t) = \sqrt{2\, std(IBI_{\Omega_t})^2 - \frac{1}{2}\, std(IBI'_{\Omega_t})^2} \tag{5}$$

where IBI′ is the derivative of IBI, std() refers to the standard deviation, and Ω_t: $t - T \leq t_i \leq t$. In this study T is fixed in 15 seconds, as per previous simulation studies in humans [26], and the validation is performed using the robust approach. In Figure 3, we provide a single-subject illustration of estimations using various time window lengths. In Figure 4, we present another example that employs the four different approaches for computation under the presence of ectopic heartbeats.

The distance to the origin R_0 and ellipse ratios SD_{01} and SD_{02} for the whole experimental duration are computed to re-center the time-resolved estimations of R, SD1 and SD2. Then, the Cardiac Parasympathetic Index (CPI) and the Cardiac Sympathetic Index (CSI), are computed as follows:

$$D(t) = \overline{R}(t) + R_0 \tag{6}$$

$$CPI(t) = k_p \cdot (\overline{SD_1}(t) + SD_{01}) + \widetilde{D}(t) \tag{7}$$

$$CSI(t) = k_s \cdot (\overline{SD_2}(t) + SD_{02}) + D(t) \tag{8}$$

where $\overline{SD_x}$ is the demeaned SD_x and $\widetilde{D}$ is the flipped D with respect the mean. The coefficients k_p and k_s define the weight of the fast and slow HRV oscillations, with respect the changes in the baseline heart rate. In this study, the values were defined as $k_p = 10$ and $k_s = 1$. Those values were chosen based on the well-stablished effects of autonomic modulations on cardiac dynamics: Sympathetic modulations primarily influence baseline heart rate [27], but also slower

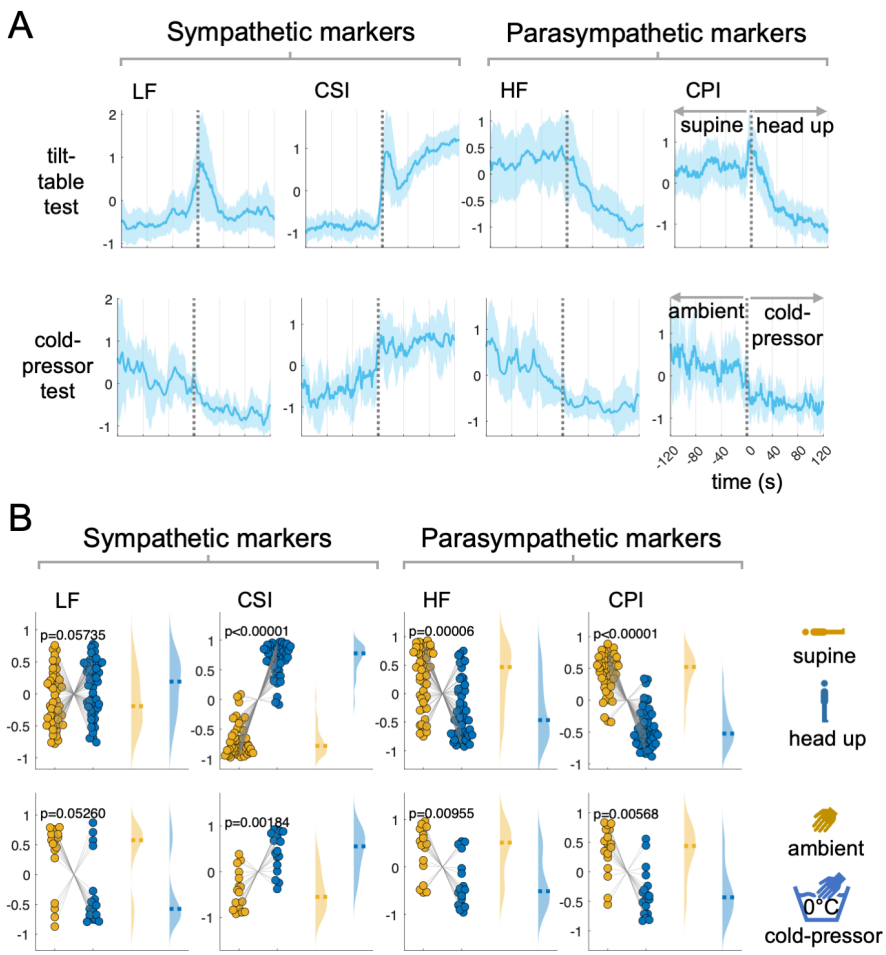

Fig. 2. Cardiac autonomic indices CSI and CPI, and their spectral counterparts LF and HF under the Tilt-table and Cold-pressor tests. The indices were used to quantify the autonomic changes triggered by the postural/temperature changes with respect to the baseline. (A) Time course of the computed indices between -120 to 120 s with respect to the condition change onset. The plot indicates the group median and the shaded areas the median absolute deviation. Time series were z-score normalized per subject before averaging for visualization purposes. (B) Statistical comparison using a signed rank Wilcoxon test, comparing the mean 120 s after the condition change with respect to the 120 s before. Dashed lines indicate the group median. All signal amplitude units are arbitrary units.

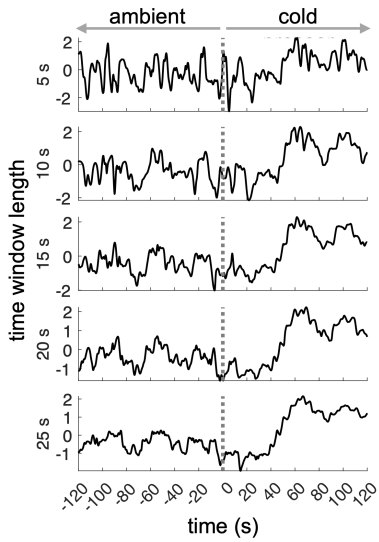

Fig. 3. Estimation of CSI (Cardiac Sympathetic Index) for one subject, for different sliding time windows. The window length displayed correspond to 5, 10, 15, 20 and 25s. The experimental condition involves the cold pressor test, with cold pressure initiating at t = 0.

HRV changes [1], while parasympathetic modulations are typically captured by quantifying faster HRV changes [1]. In Figure 5, we present an example that employs $k_p = 1, \ldots, 10$ and $k_s = 1, \ldots, 10$ for illustration.

C. Frequency-based estimation of cardiac sympathetic and parasympathetic activities

The HRV analysis in the frequency domain was computed following the adapted Wigner–Ville method for estimating the LF and HF time series [28]. The HRV series were constructed as an interbeat intervals duration time course. Consecutively, the HRV series were evenly re-sampled to 4 Hz using the spline interpolation. The pseudo-Wigner–Ville algorithm consists of a two-dimensional Fourier transform with an ambiguity function kernel to perform two-dimensional filtering, which comprises ellipses whose eccentricities depend on the parameters v_0 and τ_0, to set the filtering degrees of time and frequency domains, respectively [29]. An additional parameter λ is set to control the frequency filter roll-off and the kernel tails' size [28], [29]. The parameters are set as: $v_0 = 0.03$, $\tau_0 = 0.06$ and $\lambda = 0.3$, as per previous simulation studies [28]. Finally, low-frequency (LF) and high-frequency (HF) series were integrated withing the 0.04–0.15 Hz and 0.15–0.4 Hz, respectively [12], [13].

D. Statistical analysis

To statistically evaluate the performance of the two methods in discerning the experimental conditions, we used a two-sided non-parametric Wilcoxon signed-rank test for paired samples. The time-resolved information for all the estimated features was condensed as the average value for each experimental session, and the group-wise descriptive measures are expressed as medians and median absolute deviations (MAD). Significance was set to alpha=0.0125, following Bonferroni correction for multiple comparisons.

E. Data and code availability

All physiological data used in this study are publicly available. Postural changes and intense exercise data were gathered from Physionet [19]. Cold-pressor data were gathered from Donders Institute repository [30]. Codes implementing the methods of this study are available at https://github.com/diegocandiar/robust_hrv.

III. Results

We examined cardiac dynamics derived from HR and HRV in healthy individuals undergoing autonomic elicitation in two different conditions: tilt-table postural changes and cold-pressor test. Cardiac sympathetic and parasympathetic indices (CSI and CPI) were computed using our proposed method based on Poincaré plot descriptors of RR intervals.

The protocol on individuals undergoing postural changes consisted in transitioning from a horizontal/supine position to a vertical/head-up position using a tilt-table [20]. Our findings indicated that the proposed method precisely captured the dynamic fluctuations in autonomic activity in response to postural changes. Consistent with previous literature, we successfully observed the rise in sympathetic activity during the transition to an upright position [31]–[35], as depicted in Figure 2. Notably, when distinguishing between the two experimental conditions during postural changes, CSI and CPI exhibited superior performance compared to their spectral counterparts (Wilcoxon signed rank test, CSI: $p < 0.0001$, $Z = -6.4686$; LF: $p = 0.0574$, $Z = -1.9006$; CPI: $p < 0.0001$, $Z = 6.1341$; HF: $p < 0.0001$, $Z = 4.0051$).

The second protocol consisted on a cold-pressor test [18], in which the subjects immersed their hand in ice cold water. As shown in Figure 2, our findings revealed that variations in temperature induce alterations in autonomic activity, where an increase in sympathetic activity and a decrease in parasympathetic activity is expected [36]–[39]. While both parasympathetic markers displayed similar outcomes (Wilcoxon signed rank test, CPI: $p = 0.0057$, $Z = 2.7658$; HF: $p = 0.0096$, $Z = 2.5916$, the sympathetic markers exhibited divergent trends in relation to the experimental conditions (Wilcoxon signed rank test, CSI: $p = 0.0018$, $Z = -3.1142$; LF: $p = 0.0526$, $Z = 1.9382$). Overall, these results demonstrate that the CSI and CPI outperform their standard spectral counterparts, namely the LF and HF components, in these standard experimental conditions of autonomic elicitation.

Figure 3 presents the calculation of CSI and CPI in a subject undergoing the cold-pressor test. In this figure we highlight the impact of different time window lengths on these computations: specifically, 5, 10, 15, 20, and 25 seconds. Our findings reveal that a 5-second time window is inadequate for capturing the well-known surge in sympathetic activity induced by cold-pressure. However, a 15-second time window strikes a good balance, offering both time resolution and the ability to capture the gradual fluctuations in HRV within the 0.04-0.15 Hz range.

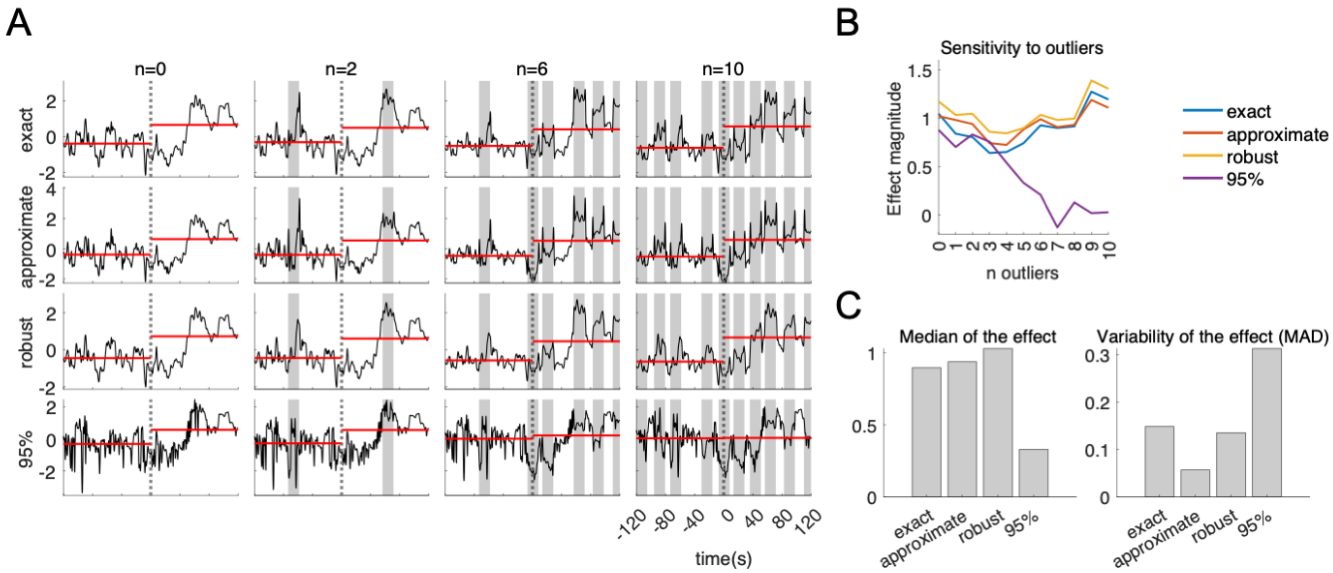

Fig. 4. Estimation of CSI (Cardiac Sympathetic Index) for one subject. (A) Each row displays the method of estimation used (exact, approximate, robust or 95%). Each column displays the result of the estimation with the presence of misdetection of R peaks from the ECG. The number of misdetections is indicated by n = 0, 2, 6, 10. The dashed line indicates the onset of the cold-pressor at t=0. Horizontal red lines indicate the CSI median before and after the cold-pressor onset. Shaded gray areas indicate the timing in which the outliers were introduced. The misdetections were introduced by adding a delay of +30 ms to the occurrence of randomly selected R peaks. (B) Effect magnitude measured as the mean CSI during the cold pressor minus the mean CSI during ambient temperature, as a function of the number of ectopic heartbeats/outliers introduced. (C). Median and Median absolute deviation (MAD) of the effect magnitude among the eleven estimations for the number of outliers n=0,1, …, 10, for each of the four approaches.

The method implementation includes four approaches of computation: "exact", "approximate", "robust", and "95%". The exact approach based on the standard covariance matrix, the approximate approach based on the short-term standard deviation computations, the robust approach based on a shrinkage covariance estimator, and the 95% approach based on a 5% outliers' rejection. The CSI estimation of one subject undergoing cold-pressure is presented in Figure 4. The estimations shown in Figure 4A correspond to the four different approaches, with each column representing the estimation results when ectopic heartbeats/outliers are externally introduced. Our findings indicate that the robust, exact, and approximate methods yield qualitatively similar estimations, with minor variations in response to the presence of ectopic heartbeats, as shown in Figure 4B. On the other hand, the 95% approach exhibits a strong resistance to outliers but results in a relatively poor overall estimation, which is demonstrated in the overall low effect magnitude (differences on CSI during the cold-pressor and baseline), but also in the high variability of the measurements with respect to the presence of outliers, as shown in Figure 4C.

For illustration, we present in Figure 5 the computation of CSI and CPI using $k_p = 1, \ldots, 10$ and $k_s = 1, \ldots, 10$. The coefficients k_p and k_s define the weight of the fast and slow HRV oscillations, with respect the changes in the baseline heart rate. Autonomic modulations on cardiac dynamics are well-documented. Sympathetic modulations primarily impact baseline heart rate [27] and also slower changes in HRV [1], while parasympathetic modulations are typically characterized by quantifying faster HRV changes [1]. In this study, we defined as $k_p = 10$ and $k_s = 1$, which represents an equal weight to heart rate and HRV for sympathetic estimations, and a higher weight to HRV for parasympathetic estimations.

IV. Discussion

We have introduced a method for the precise and time-resolved estimation of sympathetic and parasympathetic outflows in humans using ECG data. Our findings highlight the remarkable consistency of the time-resolved estimations of sympathetic and parasympathetic activities across the conditions studied. This indicates that our proposed method can accurately capture and reproduce the alterations observed in sympathetic and parasympathetic activities.

Our method uses Poincaré plots, which effectively depict the beat-to-beat alterations in heart rate, capturing both short-term and long-term fluctuations in HRV while also accounting for nonlinearities [22], [40]. Previous studies have employed Poincaré plot-derived measures to examine sympathetic and parasympathetic influences on heart rate [16], [41]–[43], including investigations into the changes observed in pathological conditions [44]–[46]. Our proposal focuses on delivering a time-resolved estimation method, enabling a comprehensive exploration of the dynamic shifts in autonomic regulations.

Physiological modeling of bodily signals plays a crucial role in uncovering the underlying aspects of autonomic dynamics by analyzing time-varying modulations of specific components. Future investigations can explore additional applications of this method, such as investigating the sympathetic and parasympathetic components involved in brain-heart dynamics [39], considering specific directionalities and latencies. Our proposed method, focusing on time-resolved estimations, facilitates a comprehensive exploration of dynamic shifts in autonomic regulations and their potential relation with ongoing brain activity [16], [39]. This approach holds particular promise for studying pathological conditions

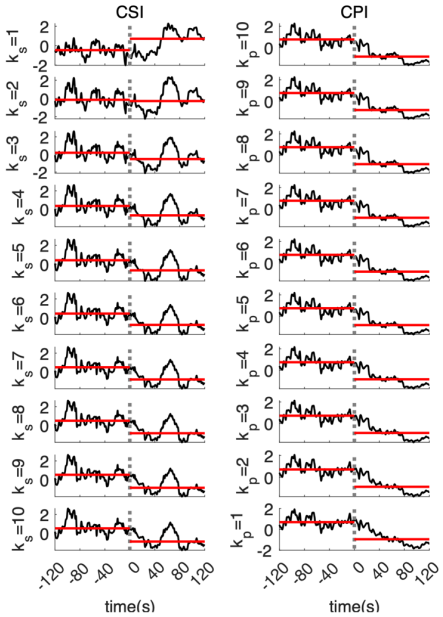

Fig. 5. Estimation of CSI (Cardiac Sympathetic Index) and CPI (Cardiac Parasympathetic Index) for a single subject. Rows display the estimation with the HR and HRV components combined, achieved by applying weights to the HRV component using the parameters 'k_s' and 'k_p' for CSI and CPI estimation, respectively. The experimental condition involves the cold pressor test, with cold pressure initiating at t = 0. Horizontal red lines indicate the CSI median before and after the cold-pressor onset

[47] given the high level of integration in within physiological networks, which highlights the significance of modeling interoceptive processes to gain insights into multisystem dysfunctions [48]. This is supported by previous research has already demonstrated the relevance of studying brain-heart interactions, as heartbeat dynamics have been implicated in various clinical applications [49].

It is worth mentioning that our method relies on the geometry of the Poincaré plot, which has been criticized due to high sensitivity to the presence of outliers and artifacts [50]. To overcome this issue, we have implemented within our method a correction of potential outliers for a robust computation of the covariance matrices [24], [25], which can be compared by the users to standard approaches through our open-source codes.

V. Conclusion

Our method holds great potential for advancing our understanding of the dynamics of sympathetic and parasympathetic fluctuations. This tool for analyzing cardiac dynamics may also contribute to the development of physiologically inspired models for the understanding of autonomic dynamics in different contexts, such as the physiological underpinnings of sensorimotor and cognitive challenge. By employing a more accurate estimation of the ongoing autonomic dynamics we can gain deeper insights into the intricate interplay within large-scale neural dynamics.

References

[1] Task Force of the European Society of Cardiology the North American Society of Pacing, "Heart Rate Variability: Standards of Measurement, Physiological Interpretation, and Clinical Use," *Circulation*, vol. 93, no. 5, pp. 1043–1065, Mar. 1996, doi: 10.1161/01.CIR.93.5.1043.

[2] U. R. Acharya, K. Paul Joseph, N. Kannathal, C. M. Lim, and J. S. Suri, "Heart rate variability: a review," *Med Biol Eng Comput*, vol. 44, no. 12, pp. 1031–1051, Dec. 2006, doi: 10.1007/s11517-006-0119-0.

[3] F. Shaffer, R. McCraty, and C. L. Zerr, "A healthy heart is not a metronome: an integrative review of the heart's anatomy and heart rate variability," *Front Psychol*, vol. 5, Sep. 2014, doi: 10.3389/fpsyg.2014.01040.

[4] M. Böhm *et al.*, "Heart rate as a risk factor in chronic heart failure (SHIFT): the association between heart rate and outcomes in a randomised placebo-controlled trial," *The Lancet*, vol. 376, no. 9744, pp. 886–894, Sep. 2010, doi: 10.1016/S0140-6736(10)61259-7.

[5] J. F. Thayer, F. Ahs, M. Fredrikson, J. J. Sollers, and T. D. Wager, "A meta-analysis of heart rate variability and neuroimaging studies: implications for heart rate variability as a marker of stress and health," *Neurosci Biobehav Rev*, vol. 36, no. 2, pp. 747–756, Feb. 2012, doi: 10.1016/j.neubiorev.2011.11.009.

[6] A. H. Kemp and D. S. Quintana, "The relationship between mental and physical health: Insights from the study of heart rate variability," *International Journal of Psychophysiology*, vol. 89, no. 3, pp. 288–296, Sep. 2013, doi: 10.1016/j.ijpsycho.2013.06.018.

[7] J. F. Thayer and E. Sternberg, "Beyond Heart Rate Variability," *Annals of the New York Academy of Sciences*, vol. 1088, no. 1, pp. 361–372, 2006, doi: 10.1196/annals.1366.014.

[8] M. Sinski, J. Lewandowski, P. Abramczyk, K. Narkiewicz, and Z. Gaciong, "Why study sympathetic nervous system?," *J. Physiol. Pharmacol.*, vol. 57 Suppl 11, pp. 79–92, Nov. 2006.

[9] M. N. Levy and P. J. Martin, "Neural Regulation of the Heart Beat," *Annual Review of Physiology*, vol. 43, no. 1, pp. 443–453, 1981, doi: 10.1146/annurev.ph.43.030181.002303.

[10] M. Brennan, M. Palaniswami, and P. Kamen, "Poincaré plot interpretation using a physiological model of HRV based on a network of oscillators," *Am. J. Physiol. Heart Circ. Physiol.*, vol. 283, no. 5, pp. H1873-1886, Nov. 2002, doi: 10.1152/ajpheart.00405.2000.

[11] H. Barcroft and H. Konzett, "On the actions of noradrenaline, adrenaline and isopropyl noradrenaline on the arterial blood pressure, heart rate and muscle blood flow in man," *J Physiol*, vol. 110, no. 1–2, pp. 194–204, Dec. 1949.

[12] B. Pomeranz *et al.*, "Assessment of autonomic function in humans by heart rate spectral analysis," *Am. J. Physiol.*, vol. 248, no. 1 Pt 2, pp. H151-153, Jan. 1985, doi: 10.1152/ajpheart.1985.248.1.H151.

[13] G. A. Reyes del Paso, W. Langewitz, L. J. M. Mulder, A. van Roon, and S. Duschek, "The utility of low frequency

heart rate variability as an index of sympathetic cardiac tone: a review with emphasis on a reanalysis of previous studies," *Psychophysiology*, vol. 50, no. 5, pp. 477–487, May 2013, doi: 10.1111/psyp.12027.

[14] R. W. de Boer, J. M. Karemaker, and J. Strackee, "Spectrum of a series of point events, generated by the integral pulse frequency modulation model," *Medical & Biological Engineering & Computing*, vol. 23, no. 2, pp. 138–142, Mar. 1985, doi: 10.1007/BF02456750.

[15] G. Valenza, L. Citi, J. P. Saul, and R. Barbieri, "Measures of sympathetic and parasympathetic autonomic outflow from heartbeat dynamics," *Journal of Applied Physiology*, vol. 125, no. 1, pp. 19–39, Feb. 2018, doi: 10.1152/japplphysiol.00842.2017.

[16] D. Candia-Rivera, "Modeling brain-heart interactions from Poincaré plot-derived measures of sympathetic-vagal activity," *MethodsX*, vol. 10, p. 102116, Mar. 2023, doi: 10.1016/j.mex.2023.102116.

[17] F. E. Rosas, D. Candia-Rivera, A. I. Luppi, Y. Guo, and P. A. M. Mediano, "Bayesian at heart: Towards autonomic outflow estimation via generative state-space modelling of heart rate dynamics." arXiv, Mar. 08, 2023. doi: 10.48550/arXiv.2303.04863.

[18] C. Varon *et al.*, "Unconstrained Estimation of HRV Indices After Removing Respiratory Influences From Heart Rate," *IEEE J Biomed Health Inform*, vol. 23, no. 6, pp. 2386–2397, Nov. 2019, doi: 10.1109/JBHI.2018.2884644.

[19] A. Mol, C. G. M. Meskers, S. P. Niehof, A. B. Maier, and R. J. A. van Wezel, "Pulse transit time as a proxy for vasoconstriction in younger and older adults," *Experimental Gerontology*, vol. 135, p. 110938, Jul. 2020, doi: 10.1016/j.exger.2020.110938.

[20] A. L. Goldberger *et al.*, "PhysioBank, PhysioToolkit, and PhysioNet: components of a new research resource for complex physiologic signals," *Circulation*, vol. 101, no. 23, pp. E215-220, Jun. 2000, doi: 10.1161/01.cir.101.23.e215.

[21] T. Heldt, M. B. Oefinger, M. Hoshiyama, and R. G. Mark, "Circulatory response to passive and active changes in posture," in *Computers in Cardiology, 2003*, Sep. 2003, pp. 263–266. doi: 10.1109/CIC.2003.1291141.

[22] J. Pan and W. J. Tompkins, "A Real-Time QRS Detection Algorithm," *IEEE Transactions on Biomedical Engineering*, vol. 32, no. 3, pp. 230–236, Mar. 1985, doi: 10.1109/TBME.1985.325532.

[23] M. Brennan, M. Palaniswami, and P. Kamen, "Do existing measures of Poincare plot geometry reflect nonlinear features of heart rate variability?," *IEEE Transactions on Biomedical Engineering*, vol. 48, no. 11, pp. 1342–1347, Nov. 2001, doi: 10.1109/10.959330.

[24] R. Sassi *et al.*, "Advances in heart rate variability signal analysis: joint position statement by the e-Cardiology ESC Working Group and the European Heart Rhythm Association co-endorsed by the Asia Pacific Heart Rhythm Society," *Europace*, vol. 17, no. 9, pp. 1341–1353, Sep. 2015, doi: 10.1093/europace/euv015.

[25] J. Schäfer and K. Strimmer, "A shrinkage approach to large-scale covariance matrix estimation and implications for functional genomics," *Stat Appl Genet Mol Biol*, vol. 4, p. Article32, 2005, doi: 10.2202/1544-6115.1175.

[26] P. J. Rousseeuw and K. V. Driessen, "A Fast Algorithm for the Minimum Covariance Determinant Estimator," *Technometrics*, vol. 41, no. 3, pp. 212–223, Aug. 1999, doi: 10.1080/00401706.1999.10485670.

[27] D. Candia-Rivera, V. Catrambone, R. Barbieri, and G. Valenza, "Integral pulse frequency modulation model driven by sympathovagal dynamics: Synthetic vs. real heart rate variability," *Biomedical Signal Processing and Control*, vol. 68, p. 102736, Jul. 2021, doi: 10.1016/j.bspc.2021.102736.

[28] G. Grassi *et al.*, "Heart rate as marker of sympathetic activity," *Journal of Hypertension*, vol. 16, no. 11, p. 1635, Nov. 1998.

[29] M. Orini, R. Bailón, L. T. Mainardi, P. Laguna, and P. Flandrin, "Characterization of dynamic interactions between cardiovascular signals by time-frequency coherence," *IEEE Trans Biomed Eng*, vol. 59, no. 3, pp. 663–673, Mar. 2012, doi: 10.1109/TBME.2011.2171959.

[30] A. H. Costa and G. F. Boudreau-Bartels, "Design of time-frequency representations using a multiform, tiltable exponential kernel," *IEEE Transactions on Signal Processing*, vol. 43, no. 10, pp. 2283–2301, Oct. 1995, doi: 10.1109/78.469860.

[31] A. Mol, C. G. M. Meskers, S. P. Niehof, A. B. Maier, and R. van Wezel, "Pulse transit time as a proxy for vasoconstriction in younger and older adults." Radboud University, Apr. 03, 2020. doi: 10.34973/TE70-X603.

[32] N. Montano, T. G. Ruscone, A. Porta, F. Lombardi, M. Pagani, and A. Malliani, "Power spectrum analysis of heart rate variability to assess the changes in sympathovagal balance during graded orthostatic tilt," *Circulation*, vol. 90, no. 4, pp. 1826–1831, Oct. 1994, doi: 10.1161/01.cir.90.4.1826.

[33] W. H. Cooke, J. B. Hoag, A. A. Crossman, T. A. Kuusela, K. U. Tahvanainen, and D. L. Eckberg, "Human responses to upright tilt: a window on central autonomic integration," *J Physiol*, vol. 517 (Pt 2), pp. 617–628, Jun. 1999, doi: 10.1111/j.1469-7793.1999.0617t.x.

[34] A. Porta, E. Tobaldini, S. Guzzetti, R. Furlan, N. Montano, and T. Gnecchi-Ruscone, "Assessment of cardiac autonomic modulation during graded head-up tilt by symbolic analysis of heart rate variability," *Am J Physiol Heart Circ Physiol*, vol. 293, no. 1, pp. H702-708, Jul. 2007, doi: 10.1152/ajpheart.00006.2007.

[35] M. Bootsma, C. A. Swenne, H. H. Van Bolhuis, P. C. Chang, V. M. Cats, and A. V. Bruschke, "Heart rate and heart rate variability as indexes of sympathovagal balance," *Am J Physiol*, vol. 266, no. 4 Pt 2, pp. H1565-1571, Apr. 1994, doi: 10.1152/ajpheart.1994.266.4.H1565.

[36] Bondar Roberta L. *et al.*, "Cerebrovascular and Cardiovascular Responses to Graded Tilt in Patients With Autonomic Failure," *Stroke*, vol. 28, no. 9, pp. 1677–1685, Sep. 1997, doi: 10.1161/01.STR.28.9.1677.

[37] R. G. Victor, W. N. Leimbach, D. R. Seals, B. G. Wallin, and A. L. Mark, "Effects of the cold pressor test on

muscle sympathetic nerve activity in humans.," *Hypertension*, vol. 9, no. 5, pp. 429–436, May 1987, doi: 10.1161/01.HYP.9.5.429.

[38] J. Cui, T. E. Wilson, and C. G. Crandall, "Baroreflex modulation of muscle sympathetic nerve activity during cold pressor test in humans," *American Journal of Physiology-Heart and Circulatory Physiology*, vol. 282, no. 5, pp. H1717–H1723, May 2002, doi: 10.1152/ajpheart.00899.2001.

[39] L. Mourot, M. Bouhaddi, and J. Regnard, "Effects of the cold pressor test on cardiac autonomic control in normal subjects," *Physiol Res*, vol. 58, no. 1, pp. 83–91, 2009.

[40] D. Candia-Rivera, V. Catrambone, R. Barbieri, and G. Valenza, "Functional assessment of bidirectional cortical and peripheral neural control on heartbeat dynamics: a brain-heart study on thermal stress," *NeuroImage*, vol. 251, p. 119023, Feb. 2022, doi: 10.1016/j.neuroimage.2022.119023.

[41] M. A. Woo, W. G. Stevenson, D. K. Moser, R. B. Trelease, and R. M. Harper, "Patterns of beat-to-beat heart rate variability in advanced heart failure," *Am Heart J*, vol. 123, no. 3, pp. 704–710, Mar. 1992, doi: 10.1016/0002-8703(92)90510-3.

[42] C. K. Karmakar, A. H. Khandoker, J. Gubbi, and M. Palaniswami, "Complex Correlation Measure: a novel descriptor for Poincaré plot," *BioMedical Engineering OnLine*, vol. 8, no. 1, p. 17, Aug. 2009, doi: 10.1186/1475-925X-8-17.

[43] D. Petković and Ž. Ćojbašić, "Adaptive neuro-fuzzy estimation of autonomic nervous system parameters effect on heart rate variability," *Neural Comput & Applic*, vol. 21, no. 8, pp. 2065–2070, Nov. 2012, doi: 10.1007/s00521-011-0629-z.

[44] S. Rahman, M. Habel, and R. J. Contrada, "Poincaré plot indices as measures of sympathetic cardiac regulation: Responses to psychological stress and associations with pre-ejection period," *International Journal of Psychophysiology*, vol. 133, pp. 79–90, Nov. 2018, doi: 10.1016/j.ijpsycho.2018.08.005.

[45] P. Contreras, R. Canetti, and E. R. Migliaro, "Correlations between frequency-domain HRV indices and lagged Poincaré plot width in healthy and diabetic subjects," *Physiol. Meas.*, vol. 28, no. 1, pp. 85–94, Nov. 2006, doi: 10.1088/0967-3334/28/1/008.

[46] G. De Vito, S. D. R. Galloway, M. A. Nimmo, P. Maas, and J. J. V. McMurray, "Effects of central sympathetic inhibition on heart rate variability during steady-state exercise in healthy humans," *Clinical Physiology and Functional Imaging*, vol. 22, no. 1, pp. 32–38, 2002, doi: 10.1046/j.1475-097X.2002.00395.x.

[47] R. A. Hoshi, C. M. Pastre, L. C. M. Vanderlei, and M. F. Godoy, "Poincaré plot indexes of heart rate variability: Relationships with other nonlinear variables," *Autonomic Neuroscience*, vol. 177, no. 2, pp. 271–274, Oct. 2013, doi: 10.1016/j.autneu.2013.05.004.

[48] R. Bailón, G. Laouini, C. Grao, M. Orini, P. Laguna, and O. Meste, "The integral pulse frequency modulation model with time-varying threshold: application to heart rate variability analysis during exercise stress testing," *IEEE Trans Biomed Eng*, vol. 58, no. 3, pp. 642–652, Mar. 2011, doi: 10.1109/TBME.2010.2095011.

[49] W. G. Chen *et al.*, "The Emerging Science of Interoception: Sensing, Integrating, Interpreting, and Regulating Signals within the Self," *Trends in Neurosciences*, vol. 44, no. 1, pp. 3–16, Jan. 2021, doi: 10.1016/j.tins.2020.10.007.

[50] K. Schiecke, A. Schumann, F. Benninger, M. Feucht, K.-J. Baer, and P. Schlattmann, "Brain-heart interactions considering complex physiological data: processing schemes for time-variant, frequency-dependent, topographical and statistical examination of directed interactions by convergent cross mapping," *Physiol Meas*, vol. 40, no. 11, p. 114001, Dec. 2019, doi: 10.1088/1361-6579/ab5050.

[51] B. Singh and D. Singh, "Ectopic beats and editing methods for Poincaré-plot-based HRV," *International Journal of Biomedical Engineering and Technology*, vol. 7, no. 4, pp. 353–364, Jan. 2011, doi: 10.1504/IJBET.2011.044414.